Inorg. Chem. **2003**, *42*, 4062–4070

Alkyl- and Aryl-Substituted Corroles. 4. Solvent Effects on the Electrochemical and Spectral Properties of Cobalt Corroles

Karl M. Kadish,*,† Jianguo Shao,† Zhongping Ou,† Claude P. Gros,‡ Frédéric Bolze,‡ Jean-Michel Barbe,‡ and Roger Guilard*,‡

Department of Chemistry, University of Houston, Houston, Texas 77204-5003, and Faculté des Sciences Gabriel, LIMSAG UMR 5633, Université de Bourgogne, 6 Boulevard Gabriel, 21000 Dijon, France

Received January 10, 2003

Solvent effects on the electrochemistry and spectroscopic properties of alkyl- and aryl-substituted corroles in nonaqueous media are reported. The oxidation and reduction of six compounds containing zero to seven phenyl or substituted phenyl groups on the macrocycle were studied in four different nonaqueous solvents (CH_2Cl_2, PhCN, THF, and pyridine) containing 0.1 M tetra-*n*-butylammonium perchlorate. Dimers were formed upon oxidation of all corroles in CH_2Cl_2, but this was not the case in the other three solvents, where either monomers or dimers were formed upon oxidation depending upon the solvent Gutmann donor number and the number or location of aryl substituents on the macrocycle. The half-wave potentials were analyzed as a function of the number of aryl substituents on the macrocycle as well as the concentration of added pyridine to PhCN solutions of the compound, and these data were combined with data from the spectroelectrochemistry experiments to determine the stoichiometry of the species actually in solution after the first oxidation or first reduction of each compound. The results of these experiments indicate that reduction of the bispyridine adduct $(Cor)Co^{III}(py)_2$ proceeds via the monopyridine complex $(Cor)Co^{III}(py)$ to give in each case the unligated cobalt(II) corrole $[(Cor)Co^{II}]^-$. In contrast, pyridine remains coordinated after electrooxidation, and the final product was characterized as $[(Cor)Co^{III}(py)_2]^+$.

Introduction

It has long been known that π-cation radicals of octaethylporphyrins (OEP) and octaethylcorroles (OEC) can form dimers in the solid state,[1−7] and several compounds of the types $[(OEP)M]_2^{2+}$ and $[(OEC)M]_2^{2+}$ have been structurally and spectroscopically characterized.[2−7] However, there has been no electrochemical characterization of these types of dimers in the case of porphyrins, and only two papers have been published on the electrochemistry of these species in the case of corroles.[8,9] The first electrochemical study showed that the electrooxidation of (OEC)M, where M = Co, Ni, or Cu, involved a reaction of dimeric species giving π-cation radicals and dications of the types $[(OEC)M]_2^{\bullet+}$ and $[(OEC)M]_2^{2+}$ in nonbinding or weakly binding media such as CH_2Cl_2 and PhCN.[8] A similar dimerization occurred for a series of alkyl- and aryl-substituted cobalt corroles in CH_2Cl_2, thus indicating that this electrode reaction was not limited to the OEC complexes but also occurred for corrole macrocycles containing the more bulky aryl substituents.[9]

In the present paper, we have extended our initial electrochemical studies of aryl-substituted cobalt corroles[9]

* Author to whom correspondence should be addressed. E-mail: kkadish@uh.edu.

† University of Houston.

‡ Université de Bourgogne.

(1) Scheidt, W. R.; Lee, Y. *Struct. Bonding* **1987**, *64*, 1.
(2) Scheidt, W. R.; Song, H.; Haller, K.; Safo, M. K.; Orosz, R. D.; Reed, C. A.; Debrunner, P. G.; Schulz, C. E. *Inorg. Chem.* **1992**, *31*, 939.
(3) Scheidt, W. R.; Cheng, B.; Haller, K.; Mislandar, A.; Rae, A. D.; Reddy, K. V.; Song, H.; Orosz, R. D.; Reed, C. A.; Cukiernik, F.; Marchon, J.-C. *J. Am. Chem. Soc.* **1993**, *115*, 1181.
(4) Schulz, C. E.; Song, H.; Lee, Y. J.; Mondal, J. U.; Mohanrao, K.; Reed, C. A.; Walker, F. A.; Scheidt, W. R. *J. Am. Chem. Soc.* **1994**, *116*, 7196.
(5) Song, H.; Rath, N. P.; Reed, C. A.; Scheidt, W. R. *Inorg. Chem.* **1989**, *28*, 1839.
(6) Van Caemelbecke, E.; Will, S.; Autret, M.; Adamian, V. A.; Lex, J.; Gisselbrecht, J. P.; Gross, M.; Vogel, E.; Kadish, K. M. *Inorg. Chem.* **1996**, *35*, 184−192.
(7) Will, S.; Lex, J.; Vogel, E.; Adamian, V. A.; Van Caemelbecke, E.; Kadish, K. M. *Inorg. Chem.* **1996**, *35*, 5577−5583.
(8) Kadish, K. M.; Adamian, V. A.; Van Caemelbecke, E.; Gueletii, E.; Will, S.; Erben, C.; Vogel, E. *J. Am. Chem. Soc.* **1998**, *120*, 11986−11993.
(9) Guilard, R.; Gros, C. P.; Bolze, F.; Jérôme, F.; Ou, Z.; Shao, J.; Fischer, J.; Weiss, R.; Kadish, K. M. *Inorg. Chem.* **2001**, 4845−4855.

10.1021/ic030010b CCC: $25.00 © 2003 American Chemical Society
Published on Web 06/03/2003

Chart 1

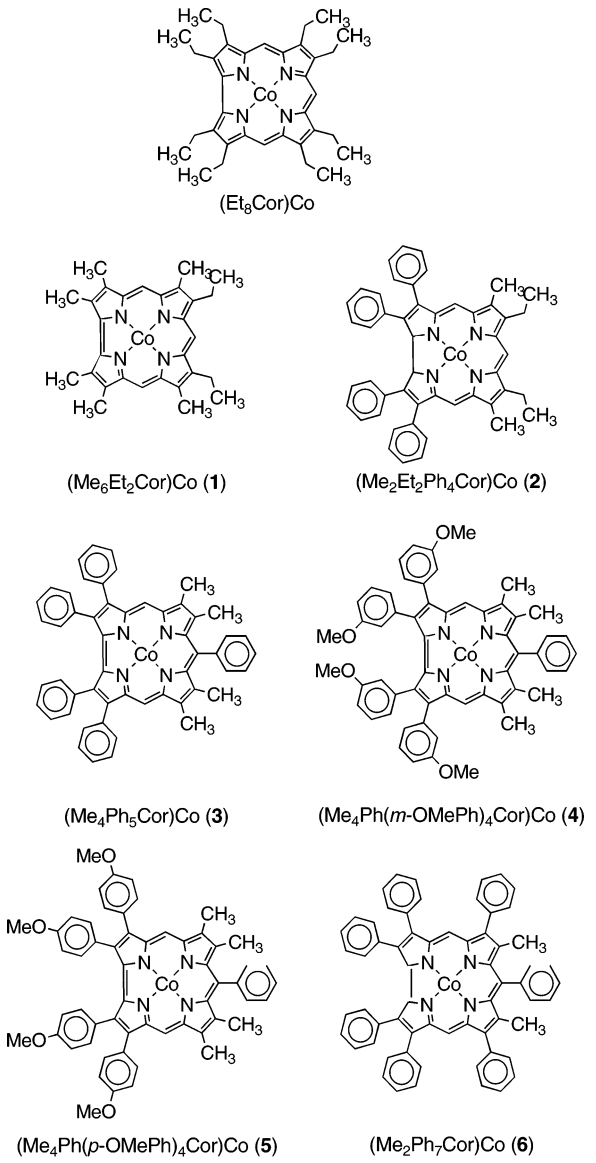

to determine how the formation of oxidized corrole dimers would vary as a function of the solvent donicity and the number or location of phenyl groups on the macrocycle. The reductive electrochemistry, UV−vis spectroscopy, and ligand binding properties of the electrogenerated Co(II) complexes were also investigated. Cyclic voltammetry and thin-layer spectroelectrochemistry were used to determine the potentials of each reaction, while the UV−vis spectra were used to evaluate the products of the electrochemical reactions under the various solution conditions. The structures of the six investigated compounds are labeled as **1**−**6** in Chart 1, which also shows the structure of $(Et_8Cor)Co$.

Experimental Section

Instrumentation. Cyclic voltammetry was carried out with an EG&G model 173 potentiostat. A three-electrode system was used and consisted of a glassy carbon or platinum disk working electrode, a platinum wire counter electrode, and a saturated calomel reference electrode (SCE). The SCE was separated from the bulk of the solution by a fritted-glass bridge of low porosity which contained the solvent/supporting electrolyte mixture. All potentials are referenced to the SCE. Solutions for electrochemical measurements under different pyridine concentrations were prepared in benzonitrile (PhCN) containing 0.1 M tetra-*n*-butylammonium perchlorate (TBAP) and 2.4×10^{-3} M $(Me_4Ph_5Cor)Co$ (**3**). The pyridine to corrole molar ratio varied from 0:1 to 1600:1.

UV−vis spectroelectrochemical experiments were performed with an optically transparent platinum thin-layer electrode of the type described in the literature.[10] Potentials were applied with an EG&G model 173 potentiostat. Time- and potential-resolved UV−vis spectra were recorded with a Hewlett-Packard model 8453 diode array rapid-scanning spectrophotometer.

Chemicals and Reagents. The investigated compounds were synthesized as described in the literature.[9] Absolute dichloromethane (CH_2Cl_2), tetrahydrofuran (THF), and pyridine (py) were obtained from Fluka Chemical Co. and used as received. PhCN was purchased from Aldrich Chemical Co. and distilled over P_2O_5 under vacuum prior to use. TBAP (Fluka Chemical Co.) was twice recrystallized from absolute ethanol and dried in a vacuum oven at 40 °C for a week before use.

Measurement of Half-Wave Potentials. Half-wave potentials were determined in most cases by cyclic voltammetry and involved a measurement of the anodic and cathodic peak potentials, which were combined using the standard equation for reversible processes given by eq 1.

$$E_{1/2} = (E_{pa} + E_{pc})/2 \quad (1)$$

Equation 1, however, could not be used for determining the reduction potentials in pyridine, where the Co(III)/Co(II) reactions were not reversible on the cyclic voltammetry time scale of 0.1−0.5 V/s and only broad "drawn out" peaks were obtained due to a potential-induced equilibrium between the bis- and monopyridine complexes in solution. Under these conditions, the values of $E_{1/2}$ could be obtained by the use of spectroelectrochemistry and of the modified Nernst equation given in eq 2, where [ox] represents the concentration of the cobalt(III) corrole in solution and [red] is the concentration of the singly reduced species as determined from measurements of UV−vis spectra obtained during the electroreduction.

$$E_{app} = E_{1/2} + (0.059/n)\log([ox]/[red]) \quad (2)$$

This method of spectrally determining half-wave potentials is well-documented in the literature[11] and involves obtaining spectra at a series of potentials where the reduction will occur and then plotting the calculated value of log([ox]/[red]) vs E_{app} to obtain $E_{1/2}$. The theoretical slope of the E_{app} vs log([ox]/[red]) plot is 0.059 V for a one-electron transfer, and the intercept at [ox] = [red] provides an accurate measurement of $E_{1/2}$.

Results and Discussion

Electrochemistry of Cobalt Corroles in Different Solvents. The electrochemical behavior of corroles **1**−**6** was investigated in four different nonaqueous solvents containing 0.1 M TBAP. Cyclic voltammograms for one of the compounds, **3**, in the four solvents are shown in Figure 1, while Figure 2 illustrates a comparison of compounds **1** and **5** in CH_2Cl_2, PhCN, and THF. The corresponding half-wave

(10) Lin, X. Q.; Kadish, K. M. *Anal. Chem.* **1985**, *57*, 1498−1501.
(11) Rohrbach, D. F.; Deutsch, E.; Heineman, W. R.; Pasternack, R. B. *Inorg. Chem.* **1977**, *16*, 2650−2652.

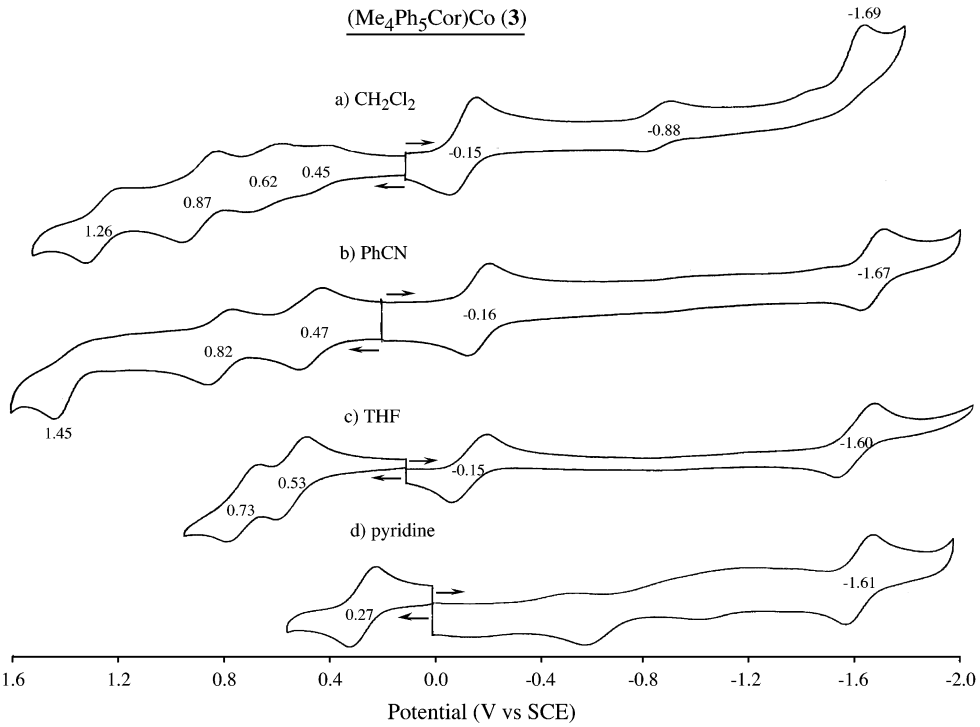

Figure 1. Cyclic voltammograms of **3** in CH_2Cl_2 (a), PhCN (b), THF (c), and pyridine (d) containing 0.1 M TBAP.

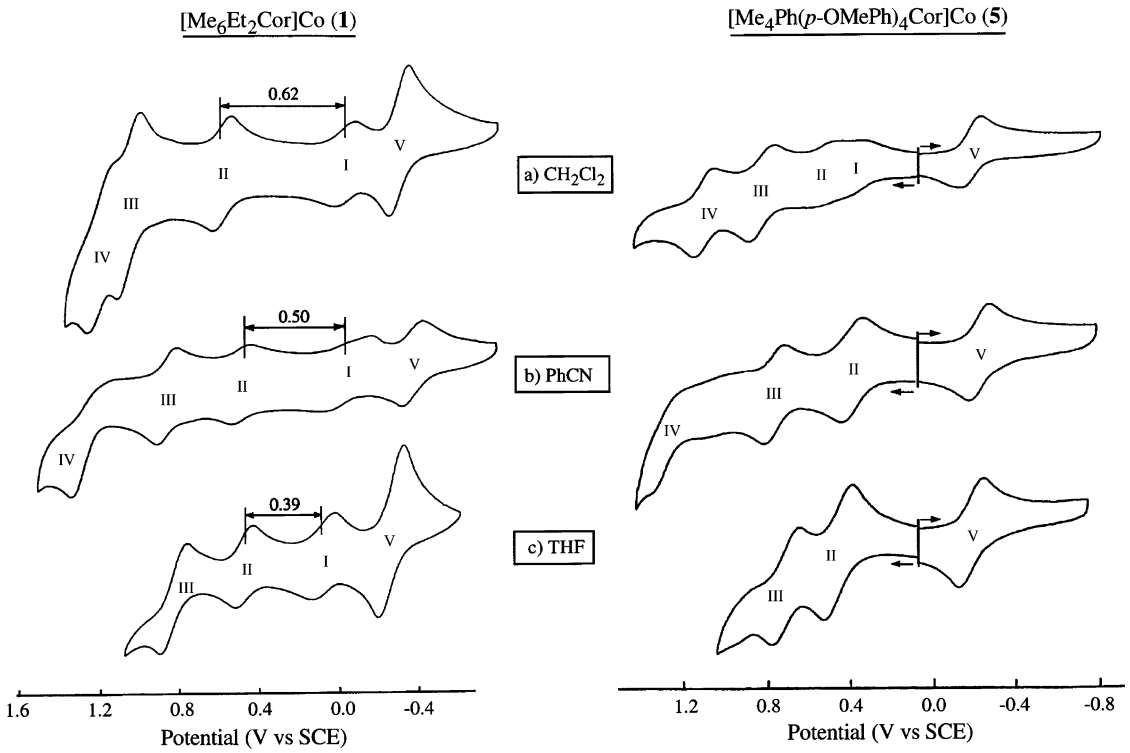

Figure 2. Cyclic voltammograms of **1** and **5** in (a) CH_2Cl_2, (b) PhCN, and (c) THF containing 0.1 M TBAP.

potentials of each process are summarized in Table 1, where the compounds are ordered according to the ease of the first oxidation and the potential separation between the first and second oxidations. For example, compound **3** has the most positive first oxidation potential of 0.45 V in CH_2Cl_2 and is listed last in the table of half-wave potentials. It undergoes four oxidations and two "major" reductions in CH_2Cl_2 (an unknown process with small peak currents is also observed in this solvent) with $E_{1/2}$ values for the four electrooxidations located at 0.45, 0.62, 0.87, and 1.26 V. The first metal-centered reduction is seen at $E_{1/2} = -0.15$ V and is followed by a second unknown reaction at $E_{1/2} = -0.88$ V (see Figure 1). This unidentified chemical reaction is not observed in the other solvents for compound **3** and is currently under continued investigation. The last reduction of **3** at $E_p = -1.69$ V is irreversible in CH_2Cl_2 but reversible in the other

Table 1. Half-Wave Potentials (V vs SCE) for Cobalt Corroles in Nonaqueous Solvents Containing 0.1 M TBAP

		ox					red	
compound	solvent	fourth	third	second	first	Δox(2−1)	first	second
(Me_6Et_2Cor)Co (**1**)	CH_2Cl_2[a]	1.21	1.07	0.59	−0.03	0.62	−0.31	b
(Et_8Cor)Co[c]		1.17	0.94	0.57	0.11	0.46	−0.30	b
($Me_2Et_2Ph_4$Cor)Co (**2**)		1.25	0.94	0.76	0.30	0.46	−0.16	−1.76[e]
(Me_2Ph_7Cor)Co (**6**)		1.26	0.84	0.52	0.34	0.18	d	−1.70[e]
(Me_4Ph(*p*-OMePh)$_4$Cor)Co (**5**)		1.15	0.87	0.55	0.38	0.17	−0.18	−1.74[e]
(Me_4Ph(*m*-OMePh)$_4$Cor)Co (**4**)		1.24	0.85	0.59	0.42	0.17	−0.15	−1.69[e]
(Me_4Ph_5Cor)Co (**3**)		1.26	0.87	0.62	0.45	0.17	−0.15	−1.69[e]
(Me_6Et_2Cor)Co (**1**)	PhCN	1.37[e]	0.90	0.50	0.00	0.50	−0.36	b
(Et_8Cor)Co[c]		1.38[e]	0.86	0.49	0.14	0.35	−0.33	b
(Me_4Ph(*p*-OMePh)$_4$Cor)Co (**5**)		1.36[e]	0.70	0.41			−0.21	−1.75
($Me_2Et_2Ph_4$Cor)Co (**2**)		1.44[e]	0.82	0.59	0.36	0.23	−0.17	−1.69
(Me_4Ph(*m*-OMePh)$_4$Cor)Co (**4**)		1.44[e]	0.71	0.46			−0.17	−1.67
(Me_4Ph_5Cor)Co (**3**)		1.45[e]	0.82	0.47			−0.16	−1.67
(Me_2Ph_7Cor)Co (**6**)		1.47[e]	0.81	0.49			−0.14	−1.63
(Me_6Et_2Cor)Co (**1**)	THF		0.85	0.50	0.11	0.39	−0.30	−1.89
(Me_4Ph(*p*-OMePh)$_4$Cor)Co (**5**)			0.74	0.49			−0.17	−1.68
($Me_2Et_2Ph_4$Cor)Co (**2**)			0.80	0.56			−0.08	−1.60
(Me_4Ph(*m*-OMePh)$_4$Cor)Co (**4**)			0.72	0.53			−0.12	−1.57
(Me_4Ph_5Cor)Co (**3**)			0.73	0.53			−0.15	−1.60
(Me_2Ph_7Cor)Co (**6**)			0.74	0.53			−0.08	−1.54
(Me_6Et_2Cor)Co (**1**)	pyridine				0.15		−0.78	−1.91[e]
(Et_8Cor)Co					0.16		−0.75	−1.95
(Me_4Ph(*p*-OMePh)$_4$Cor)Co (**5**)					0.22		−0.74[f]	−1.68
(Me_4Ph_5Cor)Co (**3**)					0.27		−0.72[f]	−1.61
(Me_4Ph(*m*-OMePh)$_4$Cor)Co (**4**)					0.28		−0.71[f]	−1.60
(Me_2Ph_7Cor)Co (**6**)					0.28		−0.70[f]	−1.60
($Me_2Et_2Ph_4$Cor)Co (**2**)					0.33		−0.72[f]	−1.61

[a] Data on compounds **1**−**6** taken from ref 9. An uncharacterized redox reduction occurs at −0.8 to −0.9 V vs SCE in CH_2Cl_2 for some of the compounds (see Figure 1). [b] Beyond the potential limit of the solvent. [c] Taken from ref 8. [d] Broad irreversible process. [e] E_p, scan rate 0.1 V/s. [f] Obtained from spectroelectrochemical experiments (see the text for details).

Scheme 1

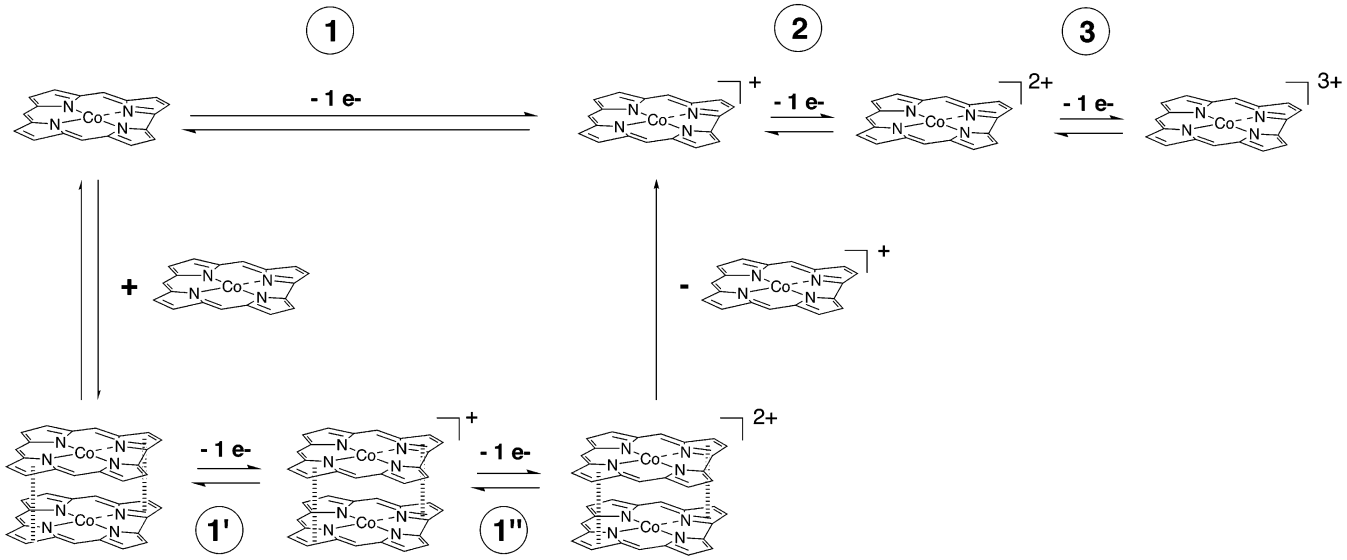

three solvents and occurs at $E_{1/2} = -1.60$ to -1.67 V as seen in Figure 1. The potential for this process is not significantly affected by the change in solvent, which can be understood by a lack of solvent binding as described later in the paper.

Of most significance in Figure 1 are the oxidations which occur via one of the two possible mechanisms shown in Scheme 1.[8,9] One mechanism involves oxidation via a dimeric species (reactions 1′ and 1″ in Scheme 1) as is seen for compound **3** in CH_2Cl_2, while the other involves oxidation of a "simple" monomeric corrole (reactions 1−3) as is seen in PhCN, THF, or pyridine.

As discussed in earlier publications,[8,9] one key diagnostic criterion for assignment of a corrole dimer in solution is that the first one-electron oxidation is split into two processes which occur at different potentials, each of which has a decreased peak current by cyclic voltammetry and involves approximately half the number of electrons transferred as compared to the first reduction, which involves a Co(III)/Co(II) process. A dimerization of compound **3** occurs in

CH_2Cl_2/0.1 M TBAP but does not occur in PhCN, THF, or pyridine as evidenced by the fact that two well-defined one-electron transfers are observed for all of the processes in these three solvents (see Figure 1). The half-wave potentials for these oxidations are located at $E_{1/2} = 0.47$ and 0.82 V in PhCN or at $E_{1/2} = 0.53$ and 0.73 V in THF and can be compared to $E_{1/2}$ values of 0.19 and 0.76 V for a similar one-electron oxidation of (OEC)Co(PPh_3) in the same solvent.[12]

Four electrooxidations are seen for all of the investigated corroles in CH_2Cl_2 (see Table 1). The peak currents for the first processes (reactions I and II) in each case are about half the peak currents for the third oxidation (reaction III) or the first reduction (reaction V), and this is shown in Figure 2 for the cases of compound **1** in CH_2Cl_2, PhCN, and THF and compound **5** in CH_2Cl_2.

Dimerization of compound **5** does not occur in PhCN, THF (Figure 2), or pyridine, where the electrooxidation involves the stepwise conversion of a monomeric corrole to a π-cation radical and dication. The electrooxidation behavior of compounds **1** and **5** in pyridine containing 0.1 M TBAP is similar to what is seen for compound **5** in PhCN or THF, where only monomers are present (Table 1). The half-wave potentials for the first one-electron oxidation of each compound in pyridine are listed in Table 1. Additional reversible oxidations could not be observed in this solvent due to the limited anodic potential window of the solvent.

The lack of corrole dimers in pyridine can be attributed to the strong binding ability of the solvent, which leads to six-coordinate complexes with binding constants of $\log K_1K_2 = 5.78-7.70$ for the investigated compounds[9] and prevents formation of the proposed $\pi-\pi$ dimer in Scheme 1. Similar electrochemical behavior is seen for all of the corroles in CH_2Cl_2, where dimers are in each case formed, and the same is true for all of the compounds in pyridine, where only monomers exist in solution. Intermediate behavior is observed in PhCN and THF, where some of the corroles form dimers and others do not depending upon the nature of the macrocycle substituents. This is discussed in the following section.

Summary of Factors Effecting the Dimerization of Electrooxidized Cobalt Corroles. The electrochemical behavior of each investigated corrole in the four different solvents is summarized in Table 2, where D and M represent the formation of a dimer or monomer oxidation product. The product of the first oxidation is in all cases a "half-oxidized dimer" in CH_2Cl_2 and in all cases a monomer in pyridine (see Scheme 1). However, in PhCN or THF, the first oxidation product (a dimer or a monomer) varies with the specific substituent on the corrole. Compounds **1**, **2**, and (Et_8-Cor)Co[8] lack a phenyl group at the 10-*meso* position of the macrocycle, and only these compounds form oxidized dimers in PhCN. (Et_8Cor)Co was not investigated in THF, but compound **1**, which has similar alkyl substituents and no phenyl substituent, was examined, and this corrole is the only to have an oxidized dimer product in THF, with the remaining compounds forming monomers in their oxidized forms.

Table 2. Product[a] upon the First Oxidation of Cobalt Corroles in Different Solvents Containing 0.1 M TBAP

compound	CH_2Cl_2 (0.0)[b]	PhCN (11.9)	THF (20.0)	pyridine (33.1)
(Me_6Et_2Cor)Co (**1**)	D	D	D	M
(Et_8Cor)Co[c]	D	D	–	M
($Me_2Et_2Ph_4$Cor)Co (**2**)	D	D	M	M
(Me_4Ph(*p*-OMePh)$_4$Cor)Co (**5**)	D	M	M	M
(Me_4Ph(*m*-OMePh)$_4$Cor)Co (**4**)	D	M	M	M
(Me_4Ph_5Cor)Co (**3**)	D	M	M	M
(Me_2Ph_7Cor)Co (**6**)	D	M	M	M

[a] D = $\pi-\pi$-radical cation dimer, M = monomer cation radical. [b] Donor number of the solvent taken from ref 18. [c] Taken from ref 8. No data were given for THF.

In an earlier paper,[9] we reported the absolute potential separation between $E_{1/2}$ values for the first and second oxidations, Δox(2−1), of each corrole dimer in CH_2Cl_2.[9] These potential differences range from 0.62 V for compound **1** to 0.17−0.18 V for compounds **3**−**6** and are also listed in Table 1. The larger Δox(2−1) values can be associated with a stronger interaction between the two equivalent redox centers in the singly oxidized compound,[8,9,13−17] and the overall data suggest the following order of interaction between the "half-oxidized" corrole dimers:

$$[\mathbf{1}]_2^+ > [Et_8Cor]_2^+ \approx [\mathbf{2}]_2^+ > [\mathbf{3}]_2^+ \approx [\mathbf{4}]_2^+ \approx [\mathbf{5}]_2^+ \approx [\mathbf{6}]_2^+$$

A similar trend is seen in PhCN (Table 1) for **1**, [(Et_8-Cor)Co]$_2$, and **2**, the only three compounds which show dimerization behavior upon oxidation in this solvent. In this regard it should be pointed out that dimerization was observed at the electrochemical concentration of 5.0×10^{-4} to 1.0×10^{-3} M but not at concentrations less than 10^{-4} M, as measured by differential pulse voltammetry (figure not shown).

The largest potential separation between the first two oxidations in PhCN is seen for compound **1**, which has a Δox(2−1) = 0.50 V. This value decreases to 0.35 V for (Et_8Cor)Co and 0.23 V for compound **2**.

The interaction between the two macrocycles in the half-oxidized corrole will depend on the solvent, the specific substituents on the macrocycle, and the axial ligand binding strength of the complex. Compounds **1**, **2**, and (Et_8Cor)Co show the highest tendency to undergo dimerization in CH_2Cl_2 and PhCN, while compounds **3**−**6** show the lowest tendency. This difference can be explained by the fact that compounds **3**−**6** each contain a phenyl group at the 10-*meso*

(12) Kadish, K. M.; Koh, W.; Tagliatesta, P.; Sazou, D.; Paolesse, R.; Licoccia, S.; Boschi, T. *Inorg. Chem.* **1992**, *31*, 2305−2313.

(13) Geiger, W. E., Connelly, N. G., Stone, F. G. A., West, R., Eds.; Academic: Orlando, FL, 1985; Vol. 24, p 89.
(14) Kotz, J. C. In *Topics in Organic Electrochemistry*; Fry, A. J., Britton, W. E., Eds.; Plenum: New York, 1986; p 95.
(15) Yap, W. P.; Durst, R. A. *J. Electroanal. Chem. Interfacial Electrochem.* **1981**, *130*, 3.
(16) Kadish, K. M.; Boulas, P.; D'Souza, F.; Aukauloo, M. A.; Guilard, R.; Lausmann, M.; Vogel, E. *Inorg. Chem.* **1994**, *33*, 471.
(17) Chang, D.; Cocolios, P.; Wu, Y. T.; Kadish, K. M. *Inorg. Chem.* **1984**, *23*, 1629.

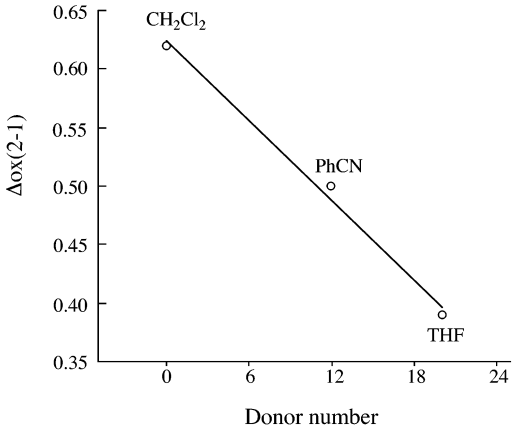

Figure 3. Relationship between the potential separation of the first two oxidations for **1** and the solvent donor number.

position of the corrole macrocycle which might hinder dimerization of the singly oxidized complex.

The variation in electrochemical behavior of the same corroles as a function of changing solvent conditions can be used to demonstrate the solvent effect on the electrooxidation mechanism. For example, cyclic voltammograms of compound **1** in Figure 2 show how the separation in half-wave potentials between the first two oxidations changes from 0.62 V in CH_2Cl_2 to 0.50 V in PhCN to 0.39 V in THF. No dimer is formed in pyridine, and here $\Delta ox(2-1)$ is essentially equal to zero. On the basis of these data, the interaction between the two macrocycles of the half-oxidized corrole dimer under different solvent conditions changes in the following order:

$$CH_2Cl_2 > PhCN > THF > pyridine$$

The occurrence of dimerization can also be related to the solvation properties of the solvent as defined by the Gutmann solvent donor number (DN).[18] As indicated in Table 2, the solvent donor number is 0.0 for CH_2Cl_2 and increases to 11.9 for PhCN and 20.0 for THF. Pyridine has the largest donor number of 33.1 among the four investigated solvents. Figure 3 illustrates a plot of the potential separation between the first two oxidations for compound **1** vs the solvent donor number. A distinct trend is obtained which suggests that the solvent effect on the electrooxidation mechanisms may depend on the binding ability of the solvent. The formation of dimers occurs more easily in solvents having the lowest donor numbers (e.g., CH_2Cl_2 and PhCN). In contrast, little or no dimerization occurs in solvents with higher donor numbers (e.g., THF or pyridine), and this can be explained in the case of pyridine by the formation of five- and six-coordinated complexes[9] which sterically hinder the possibility of stacking.

Spectroelectrochemical Results in Different Solvents. UV−vis spectroelectrochemistry was used to characterize the product of the first oxidation and first reduction of each compound and to confirm the electrooxidation mechanism illustrated in Scheme 1. Examples of the thin-layer spectra are given in Figures 4 (reduction) and 5 (oxidation) for the case of compound **3**, whose UV−vis properties in its neutral,

(18) Kadish, K. M. *Prog. Inorg. Chem.* **1986**, *34*, 437.

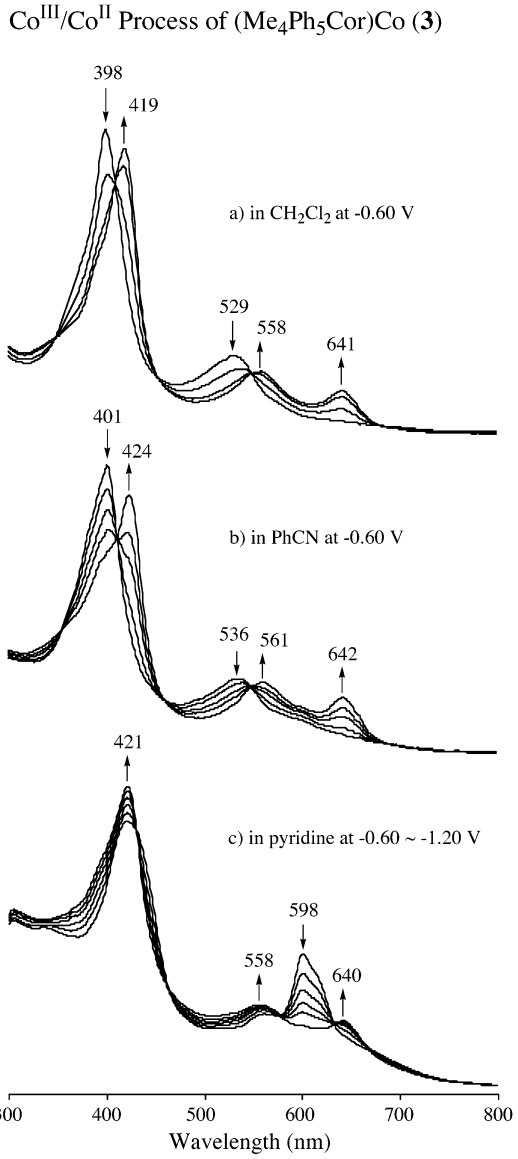

Figure 4. UV−vis spectral changes of **3** upon electroreduction at (a) −0.60 V in CH_2Cl_2, (b) −0.60 V in PhCN, and (c) −0.60 to −1.20 V in pyridine containing 0.2 M TBAP.

singly oxidized and singly reduced forms were measured in CH_2Cl_2, PhCN, and pyridine. Spectral changes upon electroreduction correspond to the Co(III)/Co(II) process in these three solvents and are illustrated in Figure 4. The neutral cobalt(III) corrole is characterized by a single absorption band in the visible region of the spectra (λ_{max} = 529 nm in CH_2Cl_2, 536 nm in PhCN, and 598 nm in pyridine), while the reduced Co(II) product has a Soret band at 419−424 nm and two well-defined visible bands which are located at 558−561 and 640−642 nm (see Figure 4). The 598 nm band in pyridine has been identified as a "marker band" of the bispyridine cobalt(III) corrole,[9,19,20] and this band disappears as the Co(III)/Co(II) process proceeds to give a cobalt(II) corrole in solution.

A key item of importance which is seen from the spectral data in Figure 4 is that virtually identical UV−vis spectra are obtained for the electrogenerated Co(II) complex in all three solvents. This strongly suggests the absence of pyridine

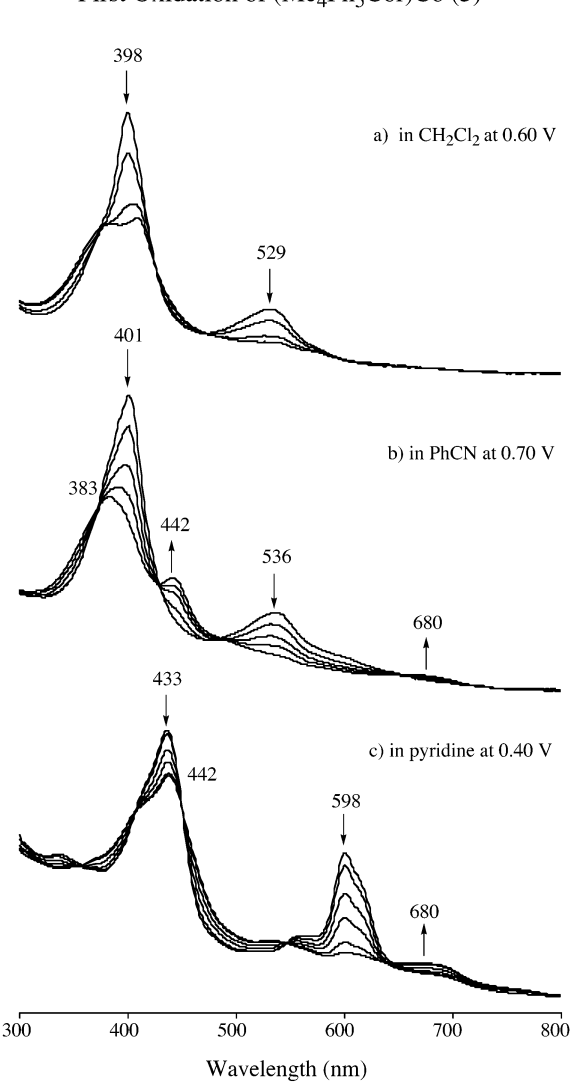

Figure 5. UV−vis spectral changes of **3** upon electrooxidation in CH_2Cl_2 (a), PhCN (b), and pyridine (c) containing 0.2 M TBAP.

binding to the reduced species in solutions of pyridine and, when combined with the electrochemical data, is consistent with the overall electrode reaction given by eq 3. As will be shown in a later section of the paper, the same electrode reaction occurs in PhCN solutions containing excess pyridine.

$$(\mathrm{Cor})\mathrm{Co}^{\mathrm{III}}(\mathrm{py})_2 + \mathrm{e}^- \rightleftharpoons [(\mathrm{Cor})\mathrm{Co}^{\mathrm{II}}]^- + 2\mathrm{py} \qquad (3)$$

The UV−vis bands of $[(Cor)Co^{II}]^-$ in CH_2Cl_2 are located at 558 and 641 nm, while in pyridine these bands are found at 558 and 640 nm (see Figure 4a,c). Thus, the overall Co(III)/Co(II) process can be written as a conversion of $(Cor)Co^{III}(py)_2$ to $[(Cor)Co^{II}]^-$, but, as discussed in the following sections, the actual reduction process proceeds via a monopyridine cobalt(III) species.

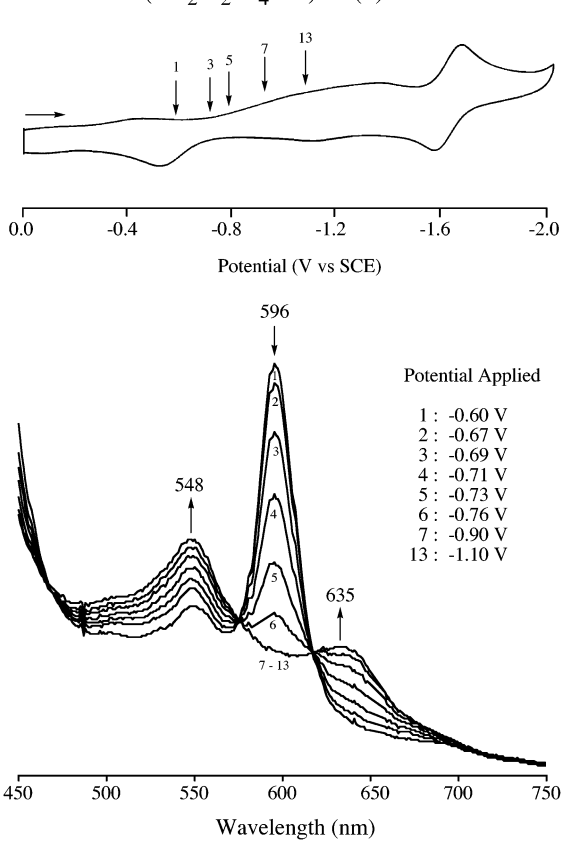

Figure 6. (a) Cyclic voltammograms of **2** in PhCN/0.1 M TBAP at a scan rate of 0.1 V/s. (b) Spectra of compound **2** at different applied potentials.

In contrast to the electroreduction, the thin-layer spectral changes which occur upon the first electrooxidation of compound **3** are different from each other in CH_2Cl_2, PhCN, and pyridine, and this is illustrated in Figure 5. The singly oxidized species in CH_2Cl_2 is formulated as the half-oxidized dimer $[\mathbf{3}]_2^+$, while the singly oxidized compound in pyridine is formulated as $[\mathbf{3}(py)_2]^+$ on the basis of data from electrochemical titrations with pyridine (see the following section). A monomeric corrole π-cation radical of compound **3** is also proposed to exist in PhCN, and this compound is characterized by bands at $\lambda = 383$ and 442 nm.

The stoichiometry of the oxidized species was not investigated in PhCN, but an absorbance at 442 nm is seen for the singly oxidized species in pyridine and may be associated in both solvents with the solvated Co(III) π-cation radical. The spectral changes upon oxidation of compound **3** in THF (figure not shown) are similar to those in PhCN, which suggests similar electrooxidation mechanisms and similar oxidation products for this compound in these two solvents.

Electrode Reactions and Determination of the Mechanism in Pyridine. Figures 6 and 7 illustrate the spectroelectrochemical method utilized for obtaining thermodynamic half-wave potentials for reduction of the cobalt(III) corroles in pyridine. The cyclic voltammetric reduction peaks are in each case drawn out and irreversible due to a potential-induced equilibrium between the $(Cor)Co^{III}(py)_2$ species

(19) Guilard, R.; Jérôme, F.; Barbe, J.-M.; Gros, C. P.; Ou, Z.; Shao, J.; Fischer, J.; Weiss, R.; Kadish, K. M. *Inorg. Chem.* **2001**, *40*, 4856−4865.
(20) Kadish, K. M.; Ou, Z. P.; Shao, J.; Gros, C. P.; Barbe, J.-M.; Jérôme, F.; Bolze, F.; Burdet, F.; Guilard, R. *Inorg. Chem.* **2002**, *41*, 3990−4005.

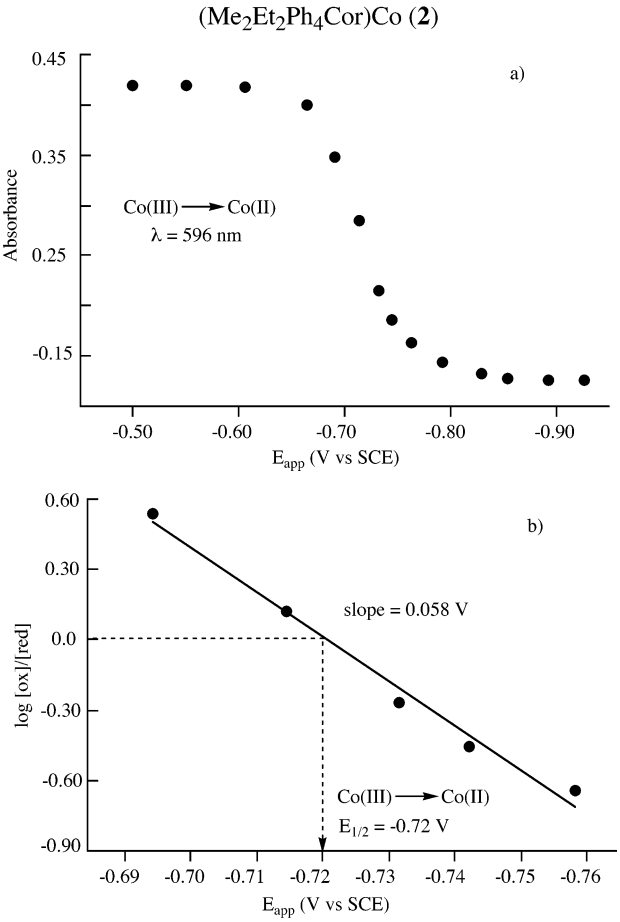

Figure 7. (a) Absorbance vs applied potential and (b) log([ox]/[red]) vs E_{app} for the Co(III)/Co(II) process of **2**.

which is actually in solution and (Cor)Co^{III}(py), the form of the complex which is more easily reduced than (Cor)Co^{III}(py)$_2$ and is formed at the electrode surface prior to electroreduction. The "ill-defined" reduction in pyridine is illustrated in Figure 1 for the case of compound **3**, and the same drawn out reduction process is also seen in Figure 6 for the case of ($Me_2Et_2Ph_4$Cor)Co (**2**). The reduction of compound **2** in a thin-layer cell at a series of progressively more negative potentials gives the resulting UV−vis spectra illustrated in the same figure. The starting species displays the characteristic bispyridine cobalt(III) corrole band at 596 nm, and the electrogenerated cobalt(II) corrole has two well-defined visible bands at 548 and 635 nm, both of which are also seen upon controlled potential reduction of the same corrole in CH_2Cl_2.[9]

A plot of the 596 nm band absorbance vs the applied potential is shown in Figure 7a, and these data were then utilized to construct a plot of log([ox]/[red]) vs applied potential which is illustrated in Figure 7b. This analysis leads to a line with a Nernstian slope of 0.058 V and an intercept of −0.72 V which is assigned as the $E_{1/2}$ for the Co(III)/Co(II) process in pyridine. This reaction is given by eq 4 and the overall reduction mechanism shown in Scheme 2.

$$(\text{Cor})\text{Co}^{\text{III}}(\text{py}) + e^- \rightleftharpoons [(\text{Cor})\text{Co}^{\text{II}}]^- + \text{py} \qquad (4)$$

Scheme 2 [a]

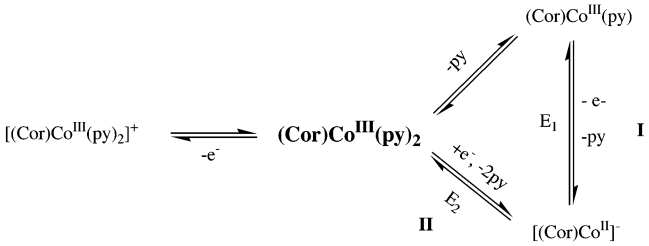

[a] E_2 is more negative than E_1; thus, process I is thermodynamically favored over process II.

Similar experiments were carried out for each corrole in pyridine, and the measured half-wave potentials are summarized in Table 1. These values range between −0.70 and −0.74 V for compounds **2**−**6**. The $E_{1/2}$ for compound **1** was evaluated as −0.78 V by cyclic voltammetry.

The assignment of (Cor)Co^{III}(py) and not Cor)Co^{III}(py)$_2$ as the species being reduced in eq 4 is based on the fact that a slow chemical reaction precedes electron transfer (a CE mechanism) as evidenced by the drawn out shape of the current−voltage curves (such as those illustrated in Figures 1 and 7). This chemical reaction preceding electron transfer could involve a dissociation of one or two axial pyridine ligands, but the dissociation of both ligands on the time scale of the experiment is highly unlikely to occur given the large binding constants ($\beta_2 > 10^7$), which strongly favor the mono- and bisligated complexes in solutions containing pyridine. The redox potentials for the Co(III)/(II) process in pyridine are much more negative than for reduction of uncomplexed (Cor)Co^{III} in CH_2Cl_2 (see the potentials in Table 1) and, when combined with the stepwise binding constants for pyridine addition to the four-coordinate complex[9] ($K_1 \cong 10^5$ and $K_2 \cong 10^2$), strongly indicate formation of (Cor)Co^{III}(py) as the electroactive species. It must be emphasized, however, that the species in solution prior to reduction is (Cor)Co^{III}(py)$_2$ and that the driving force for ligand dissociation is the more facile reduction potential of the monopyridine adduct.

The half-wave potentials for **3** were also measured in PhCN containing 0.1 M TBAP and 0.03−3.94 M pyridine, and these $E_{1/2}$ values were then plotted vs log [py] to determine the number of pyridine molecules complexed to the singly oxidized and singly reduced species. The resulting data are shown in parts a (oxidation) and b (reduction) of Figure 8. As seen in the figure, there is no dependence of the pyridine concentration on $E_{1/2}$ for oxidation, consistent with the lack of a change in coordination upon the abstraction of one electron, thus clearly indicating a conversion of (Cor)Co^{III}(py)$_2$ (the species in solution) to [(Cor)Co^{III}(py)$_2$]$^+$ as shown in Scheme 2. This contrasts with the case for reduction (Figure 8b), where the $E_{1/2}$ vs log [py] plot has a slope of −0.123 V as compared to the expected theoretical slope of −0.118 V for a one-electron reduction coupled with the loss of two pyridine ligands.[21] Thus, the electrochemical and spectroelectrochemical data (discussed earlier) are self-

(21) Kadish, K. M. In *Iron Porphyrin, Part II*; Lever, A. B. P., Gray, H. B., Eds.; Addison-Wesley Publishing Co.: London, 1983; pp 161−249.

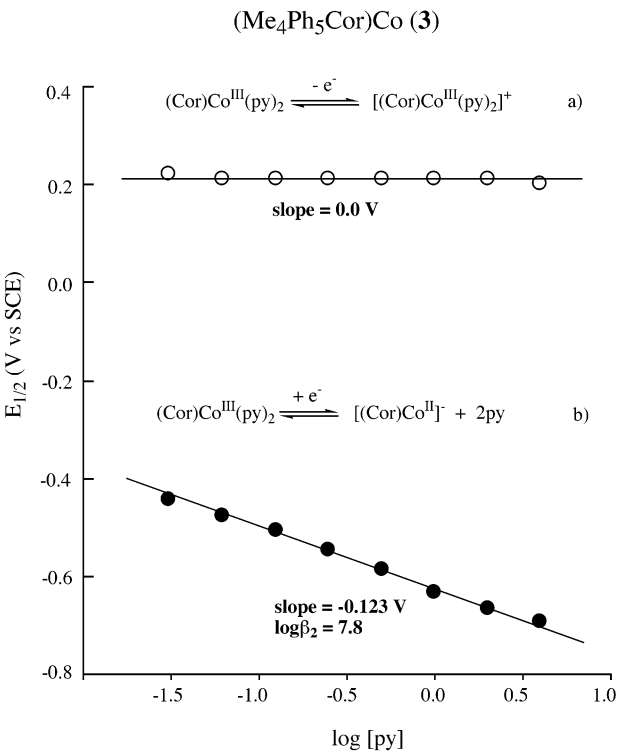

Figure 8. $E_{1/2}$ vs log [py] for the (a) first oxidation and (b) first reduction of **3** in pyridine/0.1 M TBAP.

consistent with the overall electrode reaction and can be described by eq 3.

The data in Figure 8b were also used to calculate the binding constant for the addition of two pyridine ligands to (Cor)Co^{III} using standard electrochemical equations[22] and led to a log $\beta_2 = 7.8$ in PhCN. This value compares favorably to the log $\beta_2 = 7.0$ in CH_2Cl_2 as determined earlier by UV−vis spectroscopic measurement.[9]

Summary. The electrooxidation mechanism of six corroles was examined in four different nonaqueous solvents containing 0.1 M TBAP. Dimers are invariably formed upon oxidation in CH_2Cl_2, and this contrasts with what is seen in pyridine, where only monomers are observed. The oxidation mechanism in PhCN and THF is intermediate between the two cases, and either monomers or dimers are formed depending upon the solvent Gutmann donor number and the number or location of aryl substituents on the corrole macrocycle.

The bispyridine adduct of the neutral compounds in pyridine undergoes a reversible ring-centered one-electron oxidation to form a corrole cation radical which retains the two bound pyridine axial ligands. However, the metal-centered reduction of the corrole is irreversible in pyridine and proceeds via the unreduced monopyridine adduct to give an unligated cobalt(II) corrole as the final reduction product.

Acknowledgment. The support of the Robert A. Welch Foundation (K.M.K., Grant E-680) is gratefully acknowledged. This work was supported by the French Ministry of Research (MENRT), CNRS (UMR 5633), and Air Liquide.

IC030010B

(22) Kadish, K. M.; Bottomley, L. A. *Inorg. Chem.* **1980**, *19*, 832−836.